Vol. 5: 243–258, 1995 | CLIMATE RESEARCH Clim Res | Published December 7

Synoptic scale disturbances of the Indian summer monsoon as simulated in a high resolution climate model

M. Lal[1,*], L. Bengtsson[2], U. Cubasch[1], M. Esch[2], U. Schlese[1]

[1] Deutsches Klimarechenzentrum GmbH, Bundesstraße 55, D-20146 Hamburg, Germany
[2] Max-Planck-Institut für Meteorologie, Bundesstraße 55, D-20146 Hamburg, Germany

ABSTRACT: The Hamburg atmospheric general circulation model ECHAM3 at T106 resolution (1.125° lat./lon.) has considerable skill in reproducing the observed seasonal reversal of mean sea level pressure, the location of the summer heat low as well as the position of the monsoon trough over the Indian subcontinent. The present-day climate and its seasonal cycle are realistically simulated by the model over this region. The model simulates the structure, intensity, frequency, movement and lifetime of monsoon depressions remarkably well. The number of monsoon depressions/storms simulated by the model in a year ranged from 5 to 12 with an average frequency of 8.4 yr^{-1}, not significantly different from the observed climatology. The model also simulates the interannual variability in the formation of depressions over the north Bay of Bengal during the summer monsoon season. In the warmer atmosphere under doubled CO_2 conditions, the number of monsoon depressions/cyclonic storms forming in Indian seas in a year ranged from 5 to 11 with an average frequency of 7.6 yr^{-1}, not significantly different from those inferred in the control run of the model. However, under doubled CO_2 conditions, fewer depressions formed in the month of June. Neither the lowest central pressure nor the maximum wind speed changes appreciably in monsoon depressions identified under simulated enhanced greenhouse conditions. The analysis suggests there will be no significant changes in the number and intensity of monsoon depressions in a warmer atmosphere.

KEY WORDS: High resolution climate models · Indian summer monsoon · Monsoon depressions/storms · Global warming · Climate change

INTRODUCTION

The Asian summer monsoon represents the most spectacular manifestation of regional anomalies in the general circulation of the atmosphere resulting from land-sea thermal contrasts and orographic features. Regional peculiarities assume a dominant role with respect to the monsoonal features over India and its neighbouring areas. The thermal structure of the adjoining sea areas — the Arabian Sea, the Bay of Bengal and the south Indian Ocean — and its temporal variations appear to have a modulating influence on the monsoon activity. The summer monsoon circulation over the Indian subcontinent is established towards the end of May and continues until the end of September. It accounts for over 75% of the annual rainfall over most of India. Much of the monsoon rainfall over the central plains of India is associated with the low pressure systems which develop over the north Bay of Bengal and move onto the subcontinent along a northwesterly track. It still remains a challenging task to realistically simulate these low pressure systems and the associated interannual and intraseasonal variabilities in monsoon rainfall in many climate models. This also limits our confidence in scenarios for likely climate change over the region due to an enhanced greenhouse effect.

Considerable improvement in the ability of climate models to simulate the present-day climate on regional scales has taken place in recent years with the intro-

* Visiting scientist; permanent affiliation is with the Centre for Atmospheric Sciences, Indian Institute of Technology, New Delhi-110016, India. E-mail: mlal@cas.iitd.ernet.in

duction of finer horizontal resolution and improved parameterization of physical processes. Apart from a reference control experiment, a doubled-CO_2 greenhouse forcing experiment has recently been carried out at the Max Planck Institute for Meteorology (MPIM), Germany, using a climate model at T106 horizontal resolution (1.125° lat./lon.). Bengtsson et al. (1995a, b) have demonstrated the capability of this model experiment to realistically simulate the tropical vortices. In this paper, we first examine the ability of this high resolution climate model to simulate the development and movement of monsoon low pressure vortices in Indian Seas in a control experiment, and then assess a plausible climate change scenario for the region based on simulation of enhanced greenhouse conditions.

THE MODEL

The present study is based on an analysis of data generated in experiments performed with the ECHAM3 model. ECHAM3 is the third generation General Circulation Model (GCM) used for global climate modelling investigations at the MPIM. The prognostic variables include vorticity, divergence, temperature, log surface pressure, water vapour and cloud water. The model has 19 layers in a vertical hybrid coordinate system. The integration is performed following a semi-implicit scheme with a leapfrog time filter at 12 min intervals. The physical parameterization used in ECHAM3 at T106 resolution has been developed and validated at T42 resolution (Roeckner et al. 1992, Gleckler et al. 1994). The only modification undertaken for the high resolution model run was to change the horizontal diffusion by introducing a ∇^4 smoothing operator for wave numbers shorter than 30 instead of applying a wave-number-dependent smoothing operator from wave number 15 as done for the T42 resolution model.

The parameterization of sub-grid-scale physical processes is formulated in a simplified parametric form. The radiation scheme uses a broad band formulation of the radiative transfer equations with 6 spectral intervals in the infrared spectrum and 4 in the solar spectrum (Hense et al. 1982, Rockel et al. 1991). Gaseous absorption due to water vapour, carbon dioxide and ozone is taken into account as well as scattering and absorption due to aerosols and clouds. The cloud optical properties are parameterized in terms of cloud water content, which is an explicit variable of the model.

The vertical turbulent transfer of momentum, heat, water vapour and cloud water is based upon the Monin-Obukhov similarity theory for the surface layer and the eddy diffusivity approach above the surface layer (Louis 1979). The drag and heat transfer coefficients depend on roughness length and the Richardson number, and the eddy diffusion coefficients depend on wind stress, mixing length and Richardson number which has been reformulated in terms of cloud conservative variables (Brinkop 1991). The effect of orographically excited gravity waves on the momentum budget is parameterized on the basis of linear theory and dimensional considerations (Palmer et al. 1986, Miller et al. 1989).

The parameterization of cumulus convection is based on the concept of mass flux and comprises the effect of deep, shallow as well as mid-level convection on the heat, water vapour and momentum budgets (Tiedtke 1989). Stratiform clouds are predicted per se in accordance with a cloud water equation that includes sources and sinks due to condensation/evaporation and precipitation formation both by coalescence of cloud droplets and sedimentation of ice crystals (Sundqvist 1978, Roeckner et al. 1991). Sub-grid-scale condensation and cloud formation are taken into account by specifying appropriate thresholds for relative humidity depending on altitude and static stability.

The land surface scheme considers the heat and water budgets in the soil, snow cover and land and the heat budget of permanent land and sea ice (Dümenil & Todini 1992). For further details on the ECHAM3 model, see Deutsches Klimarechenzentrum GmbH Technical Report No. 6 (DKRZ 1992). A detailed discussion of the global scale performance of this model is given in Arpe et al. (1994).

THE EXPERIMENT, REGION OF INTEREST AND DATA ANALYSIS

The findings reported in this paper are based on the data generated by the ECHAM3 global climate model described above in two 5 yr runs at T106 resolution. In the first (control) experiment, climatological sea surface temperatures averaged for the period 1979 to 1988 were prescribed as the boundary condition for simulation of the present-day climate. In addition to realistic simulation of present-day global climatology, this experiment demonstrated remarkably good agreement with the observed distribution of vortices in the tropical ocean and its typical annual variability (Bengtsson et al. 1995a). In the second experiment, sea surface temperatures, at the time of doubling of atmospheric CO_2, inferred from a transient coupled ocean-atmosphere model run at a coarser resolution (Cubasch et al. 1992) were used as the surface boundary condition. Also, the concentration of atmospheric

CO_2 was doubled for calculation of radiative fluxes in the model atmosphere. These two experiments have provided valuable insights into the feasibility of simulating hurricane-like tropical vortices in a high resolution GCM and the possible changes in their frequency and intensity in a warmer atmosphere.

The availability of standard archived data records consisting of all the basic and additionally derived climatological parameters at 12 h intervals prompted us to examine the performance of the ECHAM3 model in simulating monsoon circulation at very high resolution. We were also interested in exploring whether the cyclonic vortices developing over the Bay of Bengal during the peak summer monsoon activity over India are realistically simulated by the model.

The geographic region of interest for our data analysis was mainly confined to the area bounded within 5° to 30° N and 65° to 95° E. The total number of model grid points for this region was 672 (318 land points). Various diagnostics have been performed on the data to examine the skill of the model in simulating the summer monsoon circulation. These will be discussed in the following section ('Validation of regional climatology').

The monsoon depression, which is the most important synoptic-scale disturbance along the monsoon trough, is known to play a vital role in the spatial and temporal distribution of Indian monsoon rainfall. The cyclonic vorticity in the north Bay of Bengal, horizontal convergence in the lower levels and upward motion within the moist monsoon current lead to cloud build-up, heavy precipitation and release of latent heat, which are responsible for the development and maintenance of these monsoon depressions. We analysed the twice-daily data produced in the model simulation for the period from June to September (summer monsoon season) to identify these monsoon lows and depressions based on appropriate dynamical and physical criteria. A detailed outline of these criteria as well as the findings of our analysis will be presented below ('Simulation of synoptic-scale disturbances').

Validation of regional climatology

The south Asian summer monsoon circulation arises due to land-ocean temperature contrasts during summer and winter. The annual cycle of surface pressure has the largest amplitude over the Asian continent. Over northwest India and adjoining Pakistan, the lowest pressure occurs in July. The axis of this low surface pressure is oriented from the northwest to the southeast such that the elongated zone of low pressure, called the monsoon trough, lies along the Indo-Gangetic plains of north-central India. The western end of the trough merges with the heat low over Pakistan whereas the eastern end extends to the Bay of Bengal, where a series of monsoon depressions forms. The spatial patterns in these features of model-simulated mean sea level pressure distribution during January, April, July and October, representing the winter, pre-monsoon, monsoon and post-monsoon seasons respectively, are compared with the observed climatology in Fig. 1. It is evident from Fig. 1 that the ECHAM3 model at T106 resolution has considerable skill in reproducing the observed seasonal reversal of surface pressure, the location of the summer heat low as well as the position of the monsoon trough over the region. A further indication of how the model performs in simulating the seasonal mean sea level pressure can be obtained by correlating the model-simulated and observed spatial patterns of mean sea level pressure over the region. The correlation coefficients between the observed mean sea level pressure patterns, based on data sets for the period 1985 to 1990 analysed and compiled by the European Centre for Medium Range Weather Forecasts (ECMWF 1993) and the model-simulated mean sea level pressure patterns during winter and summer are 0.61 and 0.63 respectively. Considering that reasonable doubt exists about observed climatology over north and northeast India due to the scantness of observations from higher elevations in the Himalayas, the root mean square errors (RMSE) of 2.9 and 4.8 between the observed and model-simulated mean sea level pressure patterns in winter and summer, respectively, are considerably low.

In the tropics and particularly over the Indian subcontinent, the amplitude of the annual cycle in surface air temperature is much greater over the land than over the oceans. This results in a seasonal reversal of the land-ocean temperature gradient, which drives the monsoon circulation. In winter, the inland areas are colder. The land becomes progressively warmer and, by April, the daytime temperatures over peninsular India are on the order of 33 to 36°C. The temperature gradient to the north is gradual, while along the west coast it is quite steep (on the order of 5°C per degree longitude). In July, the summer monsoon causes extensive cloudiness and the mean temperatures in the south-central plains of India drop to about 30°C. The hottest region in July is the western margins of India, where mean temperatures of >35°C are not uncommon. The spatial range of temperature over India during July is about 9°C (Rao 1976). As is illustrated in Fig. 2, most of these seasonal features in spatial distribution of surface air temperature are realistically simulated by the model. The correlation coefficients between observed (Legates & Willmott 1990a) and model-simulated surface air temperature patterns during winter and summer are 0.84 (RMSE = 5.9) and 0.74 (RMSE = 3.9) respectively.

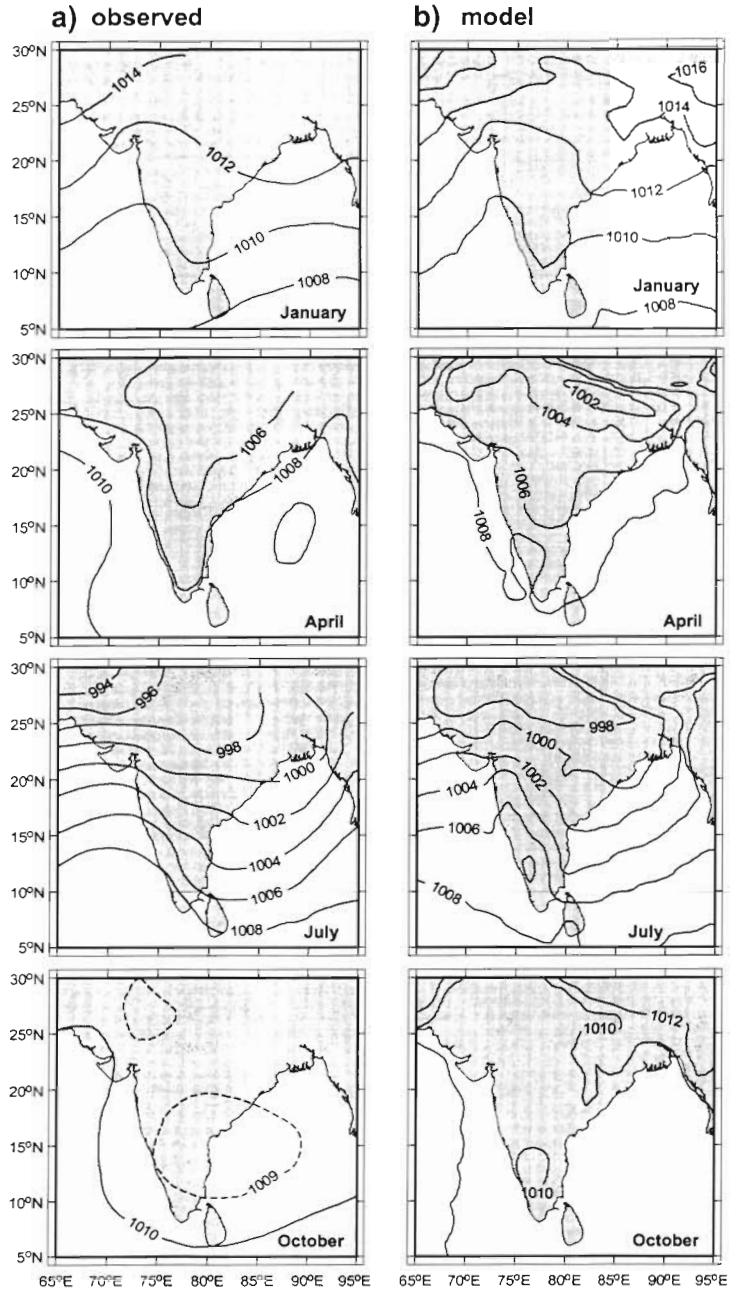

Fig. 1. Spatial distribution of mean sea level pressure (hPa) as (a) observed (Rao 1976) and (b) simulated by the model (control experiment), during January, April, July and October, representing the winter, pre-monsoon, monsoon and post-monsoon seasons, respectively, over the study area

During the monsoon season, surface winds are southwesterly over peninsular India, the Bay of Bengal and the Arabian Sea and are northeasterly in winter months (Rao 1976). In the upper troposphere, the westerly jet stream over north India shifts further north during the monsoon season and is replaced by the easterly jet stream over central and south India. A comparison of simulated mean winds for January and July over the Indian subcontinent at the 850 and 100 hPa levels reveals that these features are well captured in the model simulation. As is observed, the model simulates southwesterly winds in July with a mean speed in excess of 10 m s^{-1} over the Arabian Sea and the Bay of Bengal at 850 hPa between 5° and 20° N, while the mean wind speed over the land mass of India is about 5 m s^{-1}. The core of strong wind in the model-simulated tropical easterly jet is located between 8° and 15° N at 100 hPa, where the mean speed in July is about 27 m s^{-1} (peak winds of over 35 m s^{-1} at 100 hPa over Madras have reportedly been observed; Rao 1976). In the upper troposphere the zonal momentum produced by the Coriolis term and the east-west pressure gradient is taken out of the region by mean fluxes. The implication is that the mean meridional circulation, with southerlies in the lower levels and northerlies in the upper levels, turns into the low level westerlies and upper level easterlies by Coriolis turning The observations suggest that these low level westerlies over south India increase with height from the ground and reach a maximum between 900 and 800 hPa (Keshavamurty & Sankar Rao 1992). This feature has been realistically simulated by the model, as evidenced in the vertical cross-section of the model-simulated zonal winds (Fig. 3). The low level cross-equatorial flow and the Somali Jet that characterize the monsoon circulation are also well simulated by the model. The maximum velocity at the core of the Somali Jet is simulated ca 16 m s^{-1} as compared to 20 m s^{-1} reported in the observational records by Joseph & Raman (1966).

During pre-monsoon months, the air over most of the Indian subcontinent is very dry. Beginning in mid-May, the low level monsoon flow picks up a large amount of moisture over the east Arabian Sea. The monsoon current over the equatorial Indian Ocean and west Arabian Sea is very shallow and is overlain by dry air (Rao 1976). This shallow moist layer deepens as the monsoon current travels across the Arabian Sea and picks up moisture, and clouds develop. By July, this moist monsoon current sweeps across the entire Indian subcontinent. An examination of the model-simulated relative humidity at 850 hPa during the months of April and July (Fig. 4) suggests that the model has been able to realistically reproduce this build-up of moisture associated with monsoon circulation over the region.

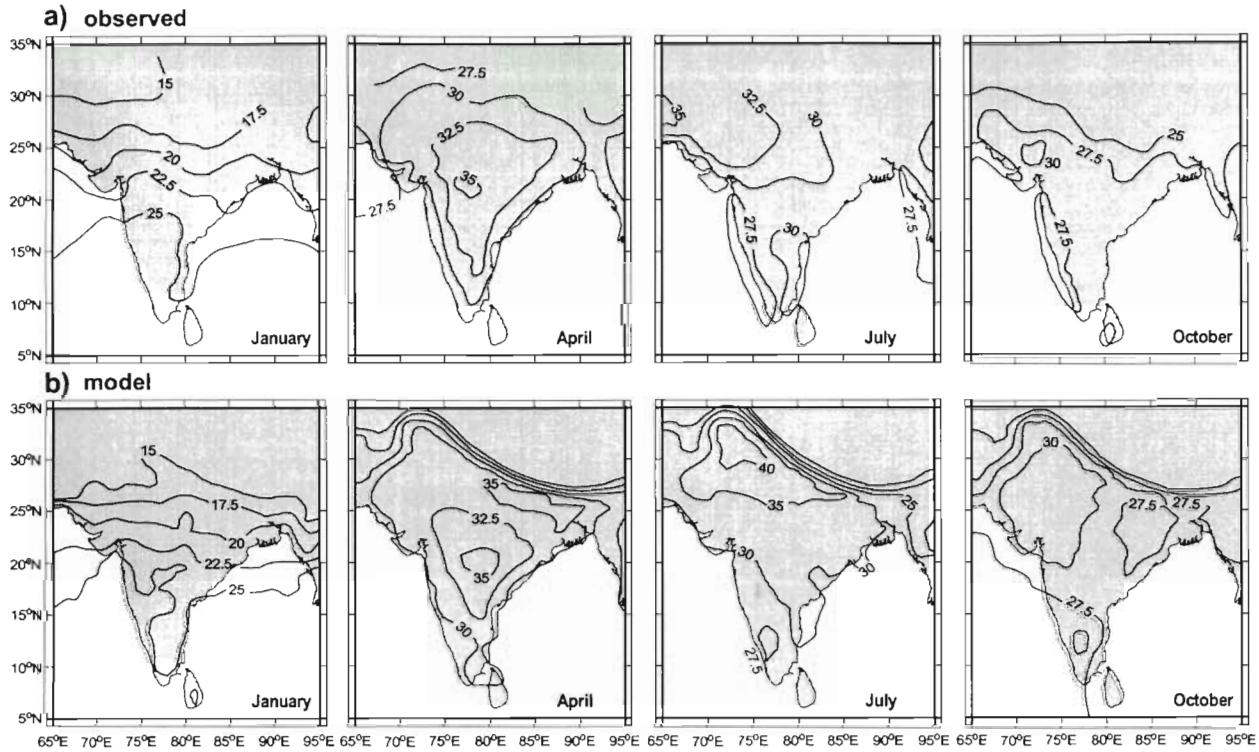

Fig. 2. Seasonal variation in surface air temperature (°C) as (a) observed (Rao 1976) and (b) simulated by the model (control experiment) over the study area

The rainfall distribution over the Indian subcontinent during the winter (December to February) and monsoon (June to September) seasons as simulated by the model is compared with observed climatology in Fig. 5. As is observed, the model simulates a steep gradient in monsoon rainfall from the west coast towards the east (a rain-shadow effect on the lee side of the Western Ghats). The striking observed variations in monsoon rainfall in the hilly and mountain ranges of northeast India are also reasonably well reproduced by the model. However, the model-simulated average total annual rainfall over the land area is 77.8 cm (averaged for 5 yr of simulation) whereas the observed mean annual rainfall is 112 cm. A total of 53.4 cm rainfall is simulated by the model for the monsoon season, while the observed mean seasonal rainfall over the region is 85 cm. The model-simulated rainfall amounts over south India in association with the northeast monsoon during winter months are in better agreement with observed records. The correlation coefficients between observed (Legates & Willmott 1990b) and model-simulated rainfall-patterns during winter and summer are

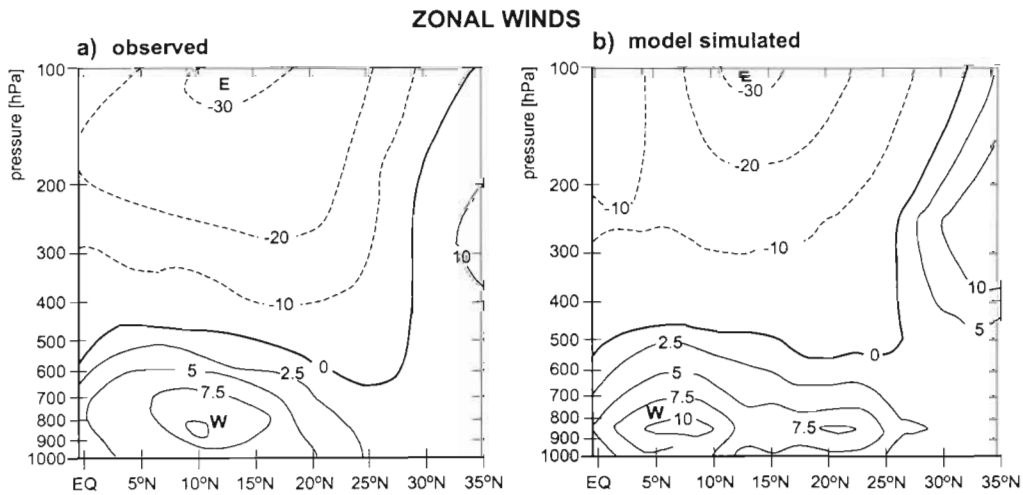

Fig. 3. Vertical cross-sections of (a) observed (after Keshavamurty & Sankar Rao 1992) and (b) model-simulated mean zonal wind (in m s^{-1}) for July, averaged between 50° and 100° E. W: westerly winds; E: easterly winds

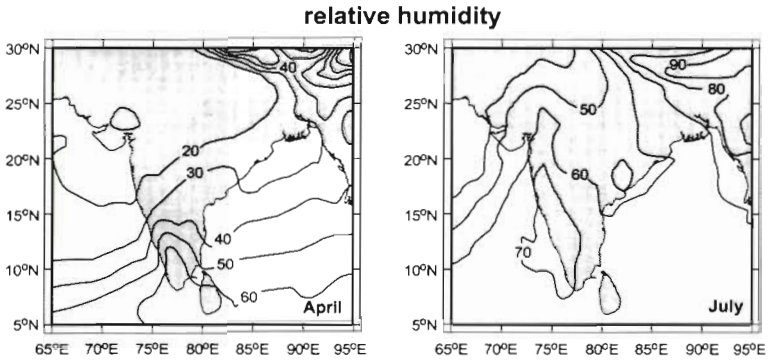

Fig. 4. The spatial distribution of model-simulated relative humidity (%) at the 850 hPa level in April and July

0.69 (RMSE = 2.0) and 0.61 (RMSE = 4.9) respectively.

An assessment of the simulation of present-day monsoon rainfall by ECHAM3 at T42 resolution, based on a 10 yr long time-slice experiment (Perlwitz et al.1993), has been reported in Lal (1993). Subsequent analysis of the present-day regional rainfall in a 30 yr long simulation with ECHAM3 at T42 resolution (Cubasch et al. 1995) has reaffirmed the findings of Lal (1993). It is interesting to note that the ECHAM3 model produces only about 65% of the total observed monsoon rainfall over the Indian subcontinent at both T42 and T106 resolutions although some improvement in terms of its spatial distribution is obtained with higher resolution as a result of better representation of regional forcings, e.g. orography, coastlines and land surface characteristics. This stresses the need for further improvements in physical parameterization of sub-grid-scale processes, e.g. cumulus convection, cloud-radiation interaction and land surface processes in climate models, particularly for tropical regions.

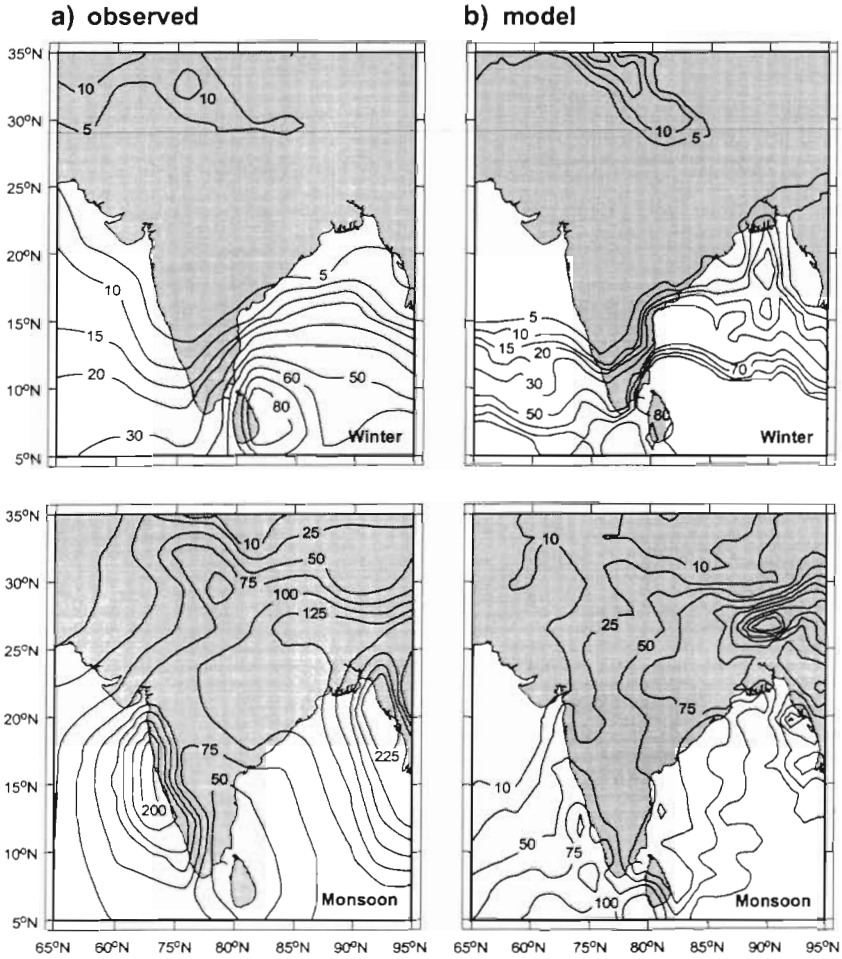

Fig. 5. Distribution of seasonal rainfall (cm) over the study area during the winter and monsoon seasons as (a) observed (Legates & Willmott 1990b) and (b) simulated by the model

Table 1. Number of observed monsoon depressions (D) and cyclonic storms (S) in Indian seas from 1891 to 1970

Location	June		July		August		September		Total no. of storms in monsoon season
	D	S	D	S	D	S	D	S	
Bay of Bengal	71	35	107	38	132	26	141	32	582
Arabian Sea	18	15	9	3	2	2	9	5	63
Land	12	1	39	1	42	–	21	1	117
Total	101	51	155	42	176	28	171	38	762
Depression/storms per year	1.3	0.6	1.9	0.5	2.2	0.4	2.1	0.5	9.5

Simulation of synoptic-scale disturbances

The number of low pressure systems over the north Bay of Bengal during the monsoon season, as well as the extent of their westward movement, are significantly related to rainfall over the central parts of India. These synoptic-scale disturbances may form *in situ* or may be linked with predecessor disturbances from the east. These disturbances are referred to as monsoon depressions when surface winds are up to 20 m s^{-1} and as cyclonic storms when higher speeds prevail. Weaker systems with wind speeds less than 10 m s^{-1} are called lows (Rao 1976). Table 1 shows the number of depressions and cyclonic storms that formed from June to September in the Bay of Bengal, Arabian Sea and over land during the 80 yr period from 1891 to 1970. There were 6 years without a depression or a cyclonic storm in July and 4 years without a depression or storm in August during this period. The number of cyclonic disturbances (depressions and cyclonic storms) per year ranged from 4 to 14 with an average frequency of about 9.5 yr^{-1}. Depressions and storms in July move mainly west to west-northwest over the Bay and across the country up to 25° N, and northwest in August (Fig. 6). In higher latitudes the movement becomes more northerly. In June and September, how-

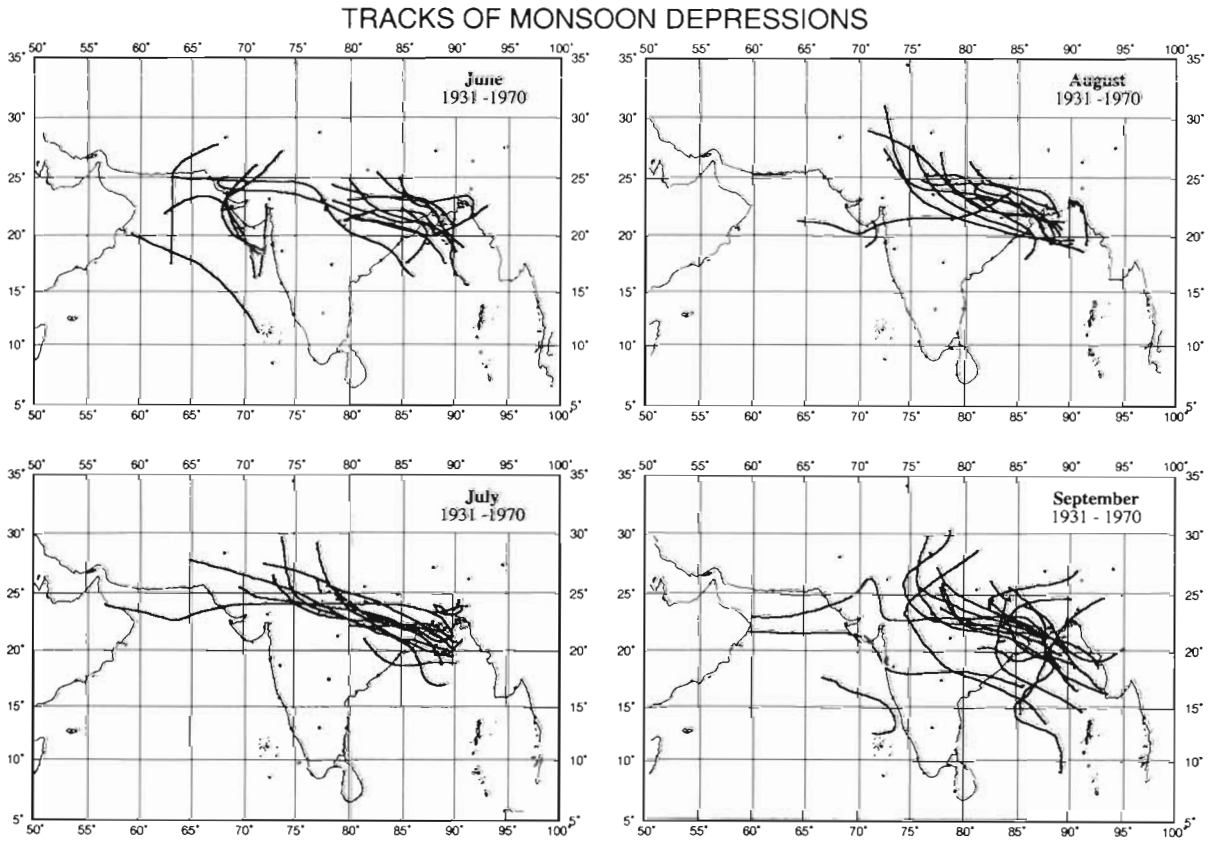

Fig. 6. Observed tracks of monsoon depressions for June to September, 1931 to 1970 (Mandal 1991)

ever, the movement is more evenly distributed, showing for example the change to a northerly course at lower latitudes, recurvature and a north or northeast course. The tangential and radial wind structure of composited monsoon depressions from 1966 to 1970 (Sikka & Paul 1975) suggests cyclonic circulation up to 1000 km in the horizontal and up to 9 km in the vertical, with anticyclonic flow aloft. The inflow is observed from the surface to 5 km and maximum outflow occurs at around 10 to 11 km. Over the northeast Arabian Sea, a cyclonic circulation within the layer from 700 to 500 hPa with only a trough in the southwesterly current is sometimes observed (Miller & Keshavamurty 1968). These systems, with maximum vorticity in the middle troposphere rather than in the surface layers, are referred to as mid-tropospheric cyclones.

The criteria for identifying development of synoptic-scale monsoon vortices over the Bay of Bengal and Arabian Sea as well as over the land region in the 5 yr of the ECHAM3 control simulation at T106 resolution were:

(1) Relative vorticity at 850 hPa $> 2.0 \times 10^{-5}$ s^{-1}.
(2) Wind speed of between 15 and 20 m s^{-1} for land depressions and >20 m s^{-1} for depressions/cyclonic storms over sea areas and a surface pressure of ≤998 hPa within a 5 × 5 grid point area which fulfilled condition 1.
(3) Minimum event duration of 2 d for a land depression/mid-tropospheric cyclone and 3.5 d for a sea depression/cyclonic storm.
(4) Along the west coast of India over the northeast Arabian Sea, if minimum surface pressure was ≤1000 hPa, but wind speed was >15 m s^{-1} and relative vorticity at 850 hPa was $>2.0 \times 10^{-5}$ s^{-1} with a peak maximum between 700 and 500 hPa for a minimum duration of 2 d, the system was identified as a mid-tropospheric cyclone.
(5) The minimum in surface pressure was identified as the centre of the depression/cyclonic storm. Mean values were calculated within a 5 × 5 grid point area around the point of minimum pressure.

Table 2 lists the number of simulated cyclonic vortices by season and month for the period of simulation. The total number of depressions/cyclonic storms forming in Indian Seas as simulated by the model over the 5 yr during the period from June to September was 41. The number of monsoon depressions/storms in a year ranged from as low as 5 to as many as 12 with an average frequency of 8.4 yr^{-1}, not significantly different from the observed climatology. The tracks of these monsoon depressions as simulated by the model in its control experiment are illustrated in Fig. 7. It was encouraging to see that almost all of the model-simulated depressions developing in July and August had a northwesterly track while the depressions forming in June and September had a tendency for northerly movement as well as recurvature, features also seen in observed storm tracks.

In order to examine the detailed structure of simulated monsoon depressions, we selected 1 case each in June and July of Years 2 and 5 respectively, as well as 2 cases in August (Years 1 and 4). The 2 storms of July (Year 1) and August (Year 5) were the most intense monsoon vortices that developed in the 5 yr of model simulation. The June storm (Year 2) formed at 15.2° N, 96.2° E on Day 4 at 12:00 h UTC with a minimum central pressure of 966 hPa and peak surface winds of 29.9 m s^{-1}. It dissipated after 9.5 d at 26.4° N, 94.5° E (the longest duration of any model-simulated monsoon depression was 13 d while the longest observed lifespan of monsoon depressions/storms developing over the north Bay of Bengal in 90 yr has been reported to be 16 d; Mandal 1991). The July storm (Year 5) formed at 23.06° N, 90.8° E (on land) on Day 4 at 12:00 h UTC with a minimum central pressure of 948 hPa and peak surface winds of 28.6 m s^{-1}. It dissipated after 9 d at 26.6° N, 70.9° E. The August depression of Year 1 was first detected at 19.13° N, 89.44° E on 28 July at 12:00 h UTC. It moved in a west northwest direction towards the east coast of India. On August 1 at 00:00 h UTC, it struck the east coast of India with a maximum surface wind of 23.8 m s^{-1} and with its centre located at

Table 2. Frequency of low pressure systems during the summer monsoon season in Indian seas as simulated in the ECHAM3 T106 control experiment. (Numbers in parentheses indicate the number of depressions which intensified into cyclonic storms)

Year	June	July	August	September	Total no. of storms per season
1	4+1[a]+1[b] (3)	3 (3)	2 (1)	1 (1)	12 (8)
2	2 (1)	2 (1)	1 (1)	1 (1)	7 (5)
3	2 (1[b])	3 (3)	3 (3)	1 (1)	9 (8)
4	–	3 (2)	–	2 (–)	5 (2)
5	1 (1)	4 (2+1[b])	3 (2)	2 (2)	10 (8)
Total no. of storms	11 (6)	15 (12)	9 (7)	7 (5)	42 (30)
Mean per year	2.5 (1.5)	3 (2.5)	1.8 (1.4)	1.2 (0.8)	8.4 (6)

[a]Mid-tropospheric cyclone over the Arabian Sea; [b]depression over the Arabian Sea

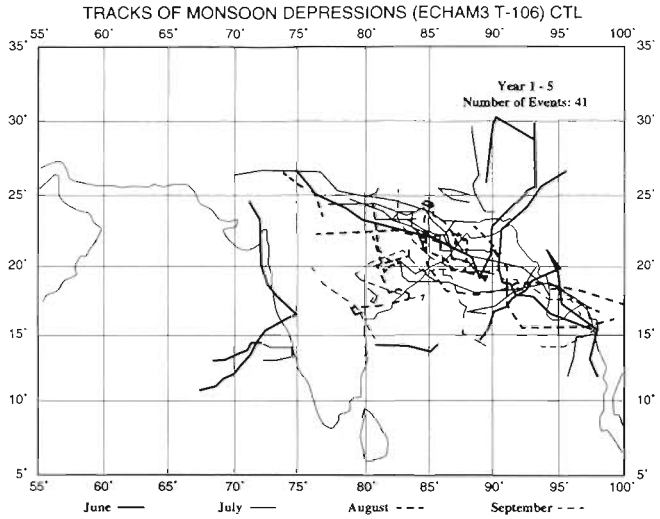

Fig. 7. Tracks of monsoon depressions for June to September simulated by the model during Years 1 to 5 of control experiment

20.87° N, 85.21° E. The lowest pressure for this depression at the time of landfall as simulated by the model was 945 hPa. The vertical structure of this storm in terms of the azimuthal mean of the tangential velocity, the radial velocity, the vorticity, the vertical velocity, surface relative humidity, vertically integrated specific humidity and rainfall at the time of landfall is depicted in Fig. 8. A land depression was observed in the model simulation on August 2 at 00:00 h UTC at 23.06° N, 77.07° E. This land depression moved on a north-northwesterly track with a central pressure of 978 hPa and a maximum surface wind speed of 22.7 m s^{-1}.

An examination of the vertical cross-sections of the tangential and radial winds associated with monsoon depressions simulated by the model suggested that the vertical extent of cyclonic circulation reached up to about the 300 hPa level, with anticyclonic flow aloft. As is observed in actual monsoon depressions (Mulki & Banerjee 1960, Godbole 1977), the horizontal extent of the cyclonic circulation was within a radius of about 5° from the depression centre. The peak tangential winds in model-simulated monsoon depressions occurred at around 850 hPa at 1.0 to 2.0° radial distance from the centre. The maximum inflow took place in the boundary layer and the maximum outflow was just above 200 hPa. Upward motions were prominent from the surface up to about 500 hPa. Vorticity was maximum between 900 and 800 hPa within a 2° radius from the centre of the storm.

The surface relative humidity in and around the model-simulated monsoon depression was above 90% and decreased sharply away from its centre. The vertically integrated specific humidity field suggests that, in association with a monsoon depression, the total moisture content of the atmosphere prior to landfall can be as high as 70 to 80 kg m^{-2}. The deep, moist monsoon environment maintains the supply of moisture required for organised cumulus convection and contributes to the relatively long life of monsoon depressions over land when compared with the typhoons and hurricanes developing in other tropical seas.

Generally, 24 h accumulated rainfall in association with a monsoon depression is 10 to 20 cm and isolated falls exceeding 30 cm in 24 h are also not uncommon (Sikka 1977). The model was able to simulate the rainfall associated with monsoon disturbances remarkably well (Fig. 8). The rainfall maxima associated with the model-simulated monsoon depressions was found to be on the order of 6 to 22 cm d^{-1} in the selected cases of

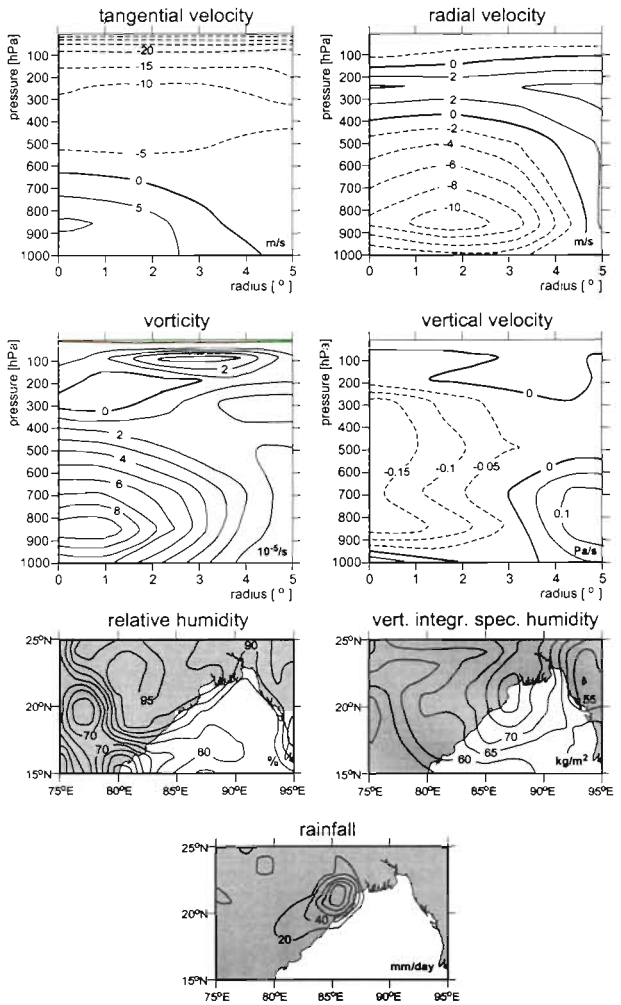

Fig. 8. Vertical cross-section of tangential and radial winds (m s^{-1}), vorticity (10^{-5} s^{-1}) and vertical velocity (Pa s^{-1}), and surface distribution of relative humidity (%), vertically integrated specific humidity (kg m^{-2}) and rainfall (mm d^{-1}) in a monsoon depression during August of Year 1 (at the time of landfall)

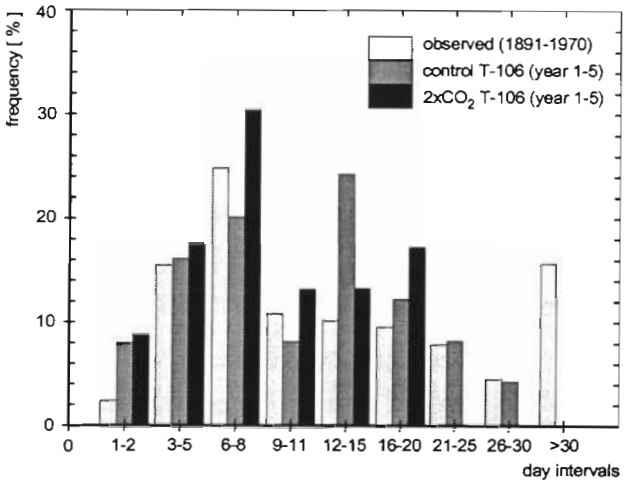

Fig. 9. Frequency distribution of the time interval between any 2 successive depressions (observed and model-simulated) during July and August

monsoon depressions discussed above. Moreover, the simulated rainfall was found to be generally higher in the southwest sector for the depressions moving northwestwardly in conformity with observational records.

An examination of various climatological aspects of synoptic disturbances forming in the north Bay of Bengal during the monsoon season shows that there was a wide scatter in the time interval between the successive formation of 2 depressions. This interval could be as small as 3 d and even exceed 1 mo (Sikka 1977). However, more depressions were formed in the interval ranging from 3 to 15 d than in the interval ranging from 16 to 30 d. A comparison of frequency distributions of the time interval between 2 successive depressions as simulated in our model and based on observed climatology during July and August is presented in Fig. 9. While the most frequently occurring time interval between 2 successive observed monsoon depressions was 6 to 8 d, the model most frequently simulated successive depressions at a time interval of 12 to 15 d.

A mid-tropospheric cyclone off the west coast of India (19.3° N, 70.7° E) was identified in the model-simulated data in Year 1 on June 26 at 00:00 h UTC. The surface pressure at the centre of this system was 998 hPa and the maximum surface wind was 16.1 m s^{-1}. An examination of the vorticity and vertical velocity associated with this system indicated that the peak vorticity was confined to a region close to the 700 hPa level while the maximum vertical velocity occurred between 700 and 500 hPa levels (Fig. 10). The vertical thermal structure at the centre of this mid-tropospheric cyclone suggested that it was cold-cored at 700 hPa and warm-cored at 500 hPa. This is in fair agreement with the observations of Miller & Keshavamurty (1968). The system moved northeastwardly with a maximum wind speed of 16.3 m s^{-1} and produced a peak rainfall of 38 mm d^{-1} before dissipating after 2.5 d.

The model also simulated the interannual variability in the formation of depressions over the north Bay of Bengal during the summer monsoon season. As is evident from Table 2, the total number of depressions simulated by the model varied from 5 in Year 4 to 12 in Year 1. A closer look at the model-simulated data suggests that a lower number of monsoon depressions in a particular year could be attributed to the predominantly sinking motion enforced by large scale convection altering the normal pattern of the Hadley-Walker cell over the region. As is evident from spatial patterns of velocity potential (a measure of divergent and convergent centres of action) at 850 and 250 hPa in Years 1 and 4 (Figs. 11 & 12), the upper level divergence and lower level convergence were much less pronounced in Year 4 relative to Year 1 over the north Bay of Bengal, which was reflected in the comparative rarity of monsoon depressions.

It is evident from the above that the ECHAM3 model has substantial skill in simulating the present-day climate and its seasonal cycle over the monsoon region at T106 resolution. The model simulated the structure, intensity, frequency, movement and duration of monsoon depressions quite realistically. In the next section, we discuss the implications of a doubling of atmospheric CO_2 for monsoon climatology in general and for the monsoon disturbances in particular.

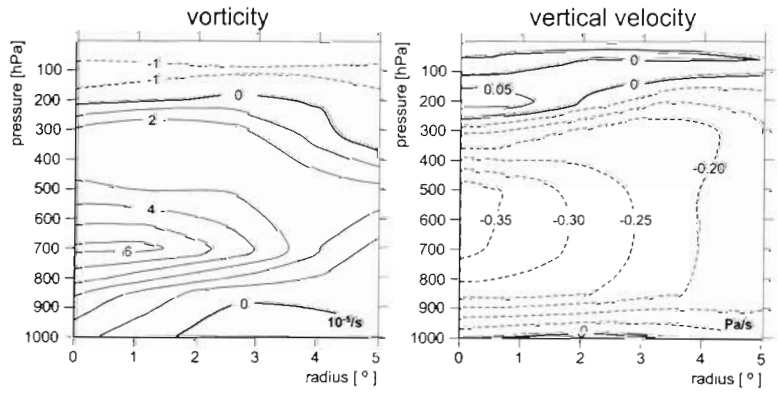

Fig. 10. Vertical cross-section of vorticity (10^{-5} s^{-1}) and vertical velocity (Pa s^{-1}) in a model-simulated mid-tropospheric cyclone (June 26, Year 1)

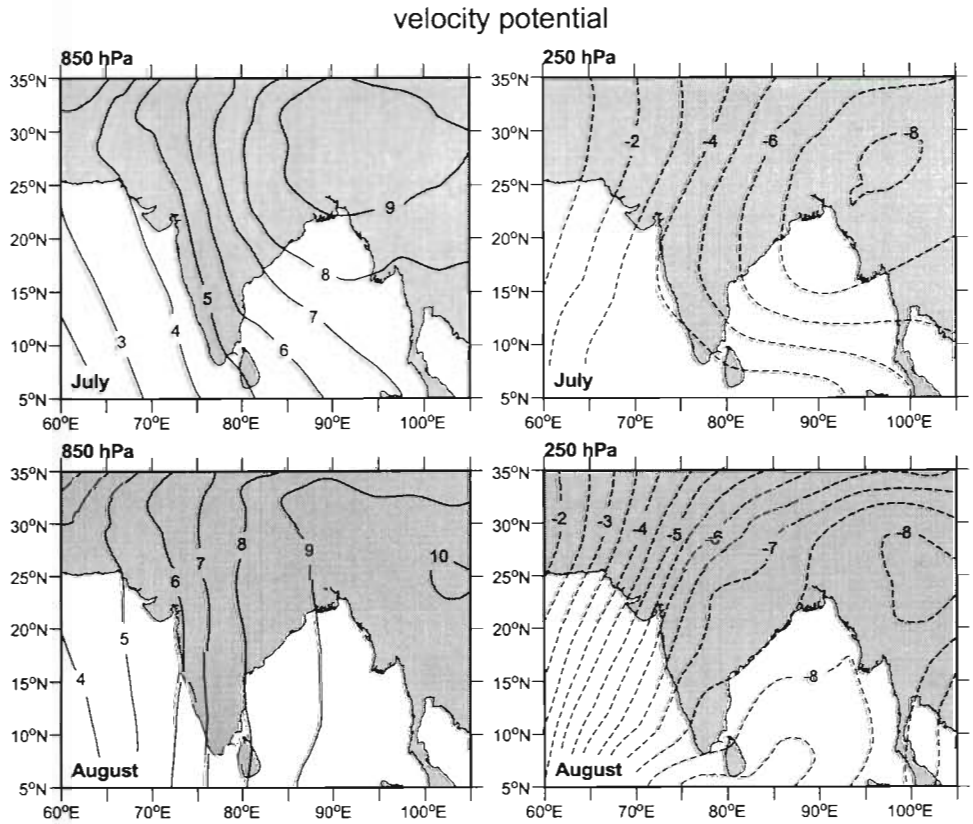

Fig. 11 Velocity potential ($km^2\ s^{-1}$) at 850 hPa and 250 hPa in July and August of Year 4, when a small number of monsoon depressions formed in the model control experiment

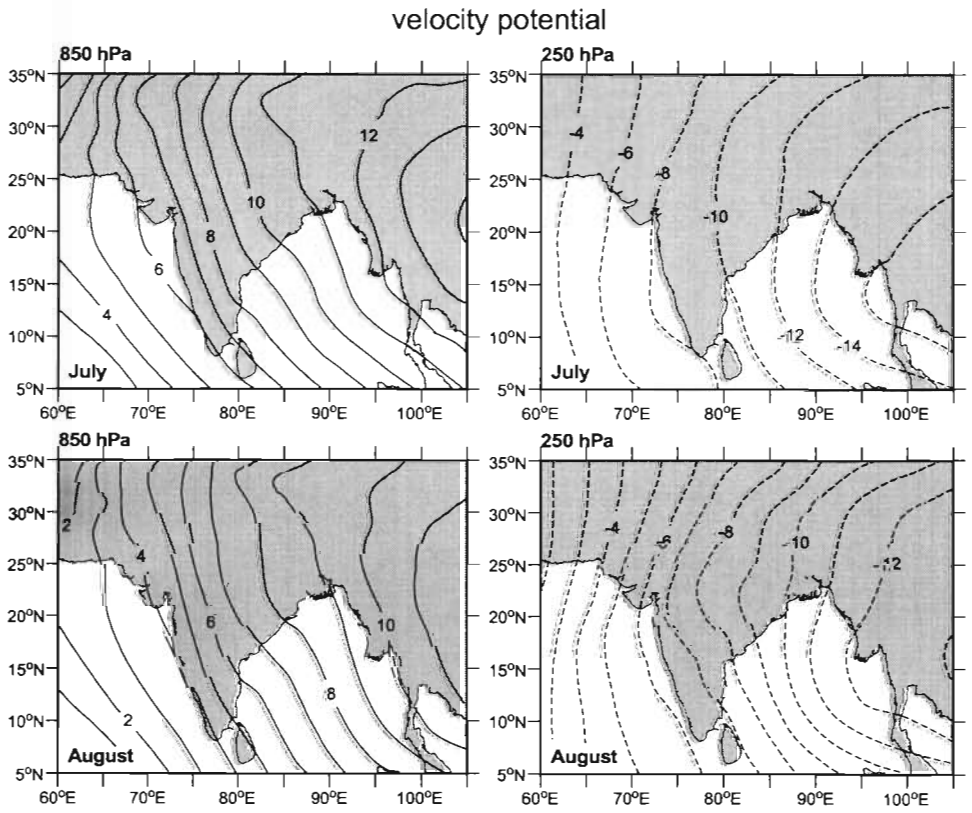

Fig. 12. Velocity potential ($km^2\ s^{-1}$) at 850 hPa and 250 hPa in July and August of Year 1, when a large number of monsoon depressions formed in the model control experiment

Climate change scenario: doubled CO_2 experiment

The ECHAM3 model at T106 resolution simulates a rise in global mean surface air temperature 1.5°C on an annual mean basis under doubled CO_2 conditions. This is marginally higher (by 0.17°C) than the surface air temperature change simulated by the coupled atmosphere-ocean climate model (ECHAM1+ LSG) in a transient experiment using the 'Business As Usual' CO_2 scenario of the IPCC at the time of CO_2 doubling (cf. Cubasch et al. 1992). The annual mean global rise in surface temperature over land regions only is 2.3°C. The greenhouse-gas-induced annual mean surface air temperature increase for the monsoon region under study is 1.7°C, slightly more than the global mean temperature rise. The annual mean surface air temperature increase over land regions of the Indian subcontinent is 2.0°C, marginally lower than the global mean surface warming. Under doubled CO_2 conditions the surface air temperature increase over the Indian subcontinent is most pronounced in winter months, when it reaches about 2.5°C. During the monsoon season, the increase in surface air temperature is 1.6°C (the minimum).

The spatial pattern of surface air temperature increase over the Indian subcontinent suggests that, on an annual mean basis, the most pronounced warming will occur over the drier semi-arid regions of northwest India. The model-simulated annual mean surface warming is close to about 1.0°C over peninsular India and about 2.0°C over central and northeast India (Fig. 13). During the monsoon season, the surface air temperature rise is significantly less over the central plains of India as compared to other regions and even a marginal cooling is simulated over one isolated region (Fig. 14). The warming over both the Arabian Sea and the Bay of Bengal is ≤1.0°C.

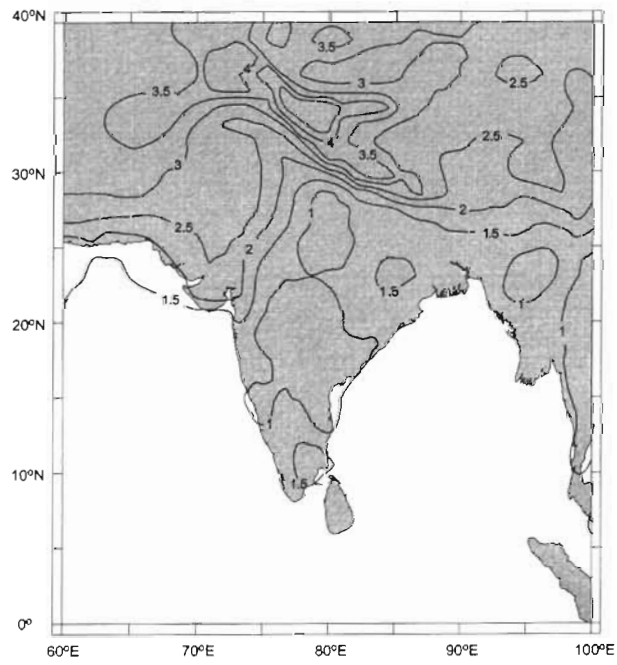

Fig. 13. Spatial pattern of change in annual mean surface air temperature (°C) over the Indian subcontinent due to doubling of CO_2 as simulated by the model

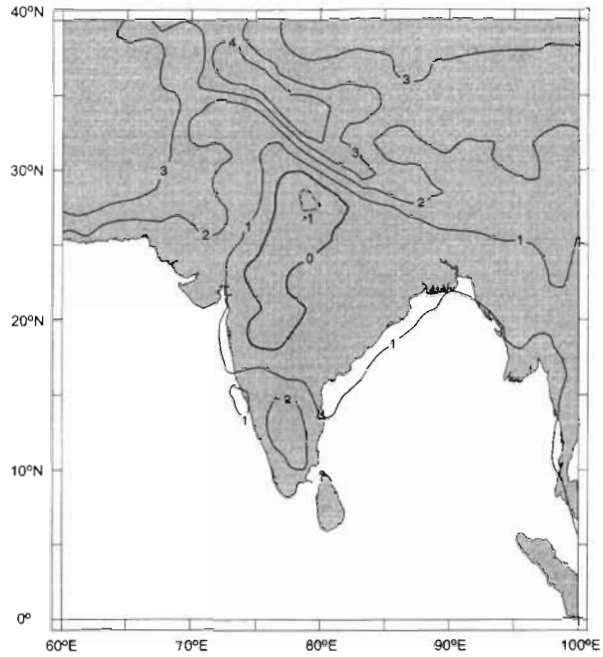

Fig. 14. Spatial pattern of change in surface air temperature (°C) during monsoon season over the Indian subcontinent due to doubling of CO_2 as simulated by the model

The model simulation suggests an increase in annual mean rainfall of 0.47 mm d^{-1} (~15%) over the land regions of the Indian subcontinent under enhanced CO_2 conditions. The increase in rainfall is largely confined to the monsoon season when the central plains of India may receive as much as 4 to 5 mm excess rainfall d^{-1} (Fig. 15). During winter, no appreciable change in rainfall over the Indian subcontinent is simulated by the model. A significant increase in post-monsoon-season rainfall is simulated along the east coast of India and coastal regions of Bangladesh.

The increase in monsoon rainfall over the Indian subcontinent simulated by the model under doubled CO_2 conditions suggests the likelihood of an enhancement in convective activity over the region. Does this mean that more monsoon depressions are likely to form over the north Bay of Bengal in a warmer atmosphere? We examined the frequency and movement of monsoon depressions forming in the north Bay of Bengal in the model-simulated data,

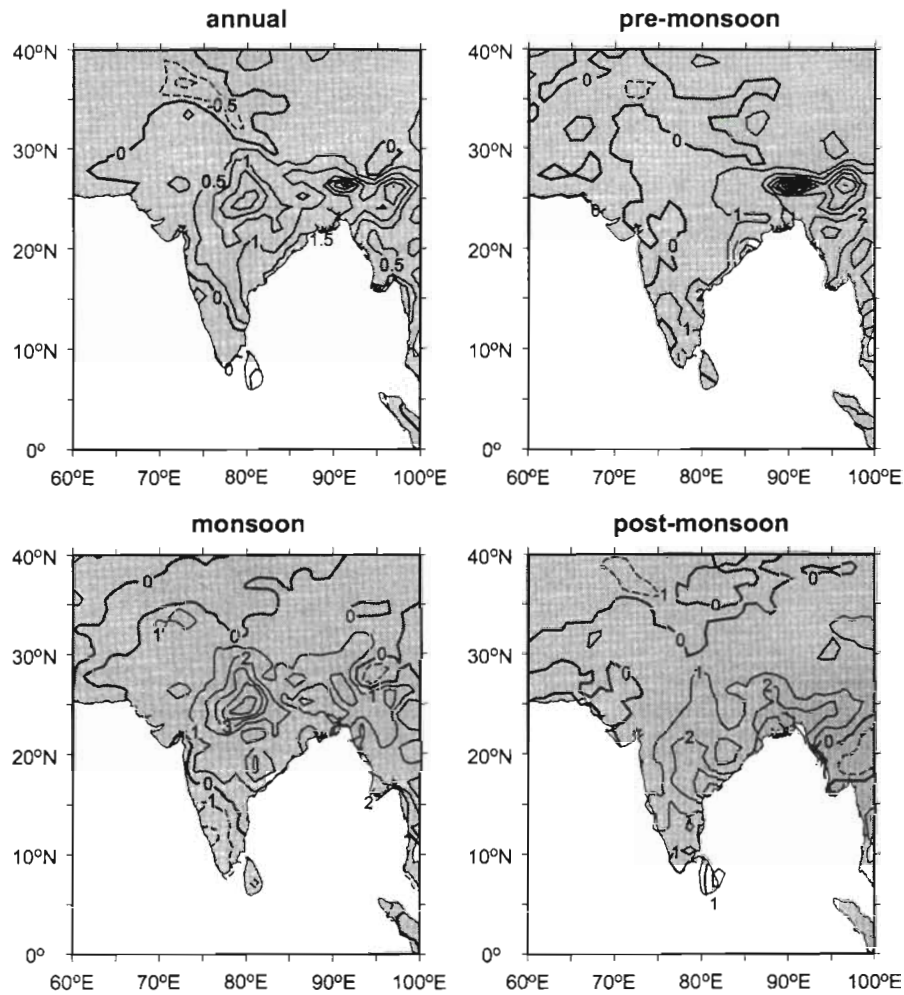

Fig. 15. Spatial patterns of change in annual and seasonal rainfall (mm d^{-1}) over the Indian subcontinent due to doubling of CO_2 as simulated by the model

following the same criteria as used in control experiment. Table 3 lists the number of simulated cyclonic vortices by season and month for the period of simulation. The total number of depressions/cyclonic storms forming in Indian seas as simulated by the model over 5 yr during the period from June to September is 38. The number of monsoon depressions/storms per year ranged from as low as 5 to as many as 11 with an average frequency of 7.6 yr^{-1}, not significantly different from the frequencies inferred in the control experiment. It is interesting to note, however, that fewer depressions formed in the month of June under doubled CO_2 conditions. Moreover, over the Arabian Sea, only 1 depression formed in the

Table 3. Frequency of low pressure systems during the summer monsoon season in Indian seas as simulated in the ECHAM3 T106 2×CO_2 experiment. (Numbers in parentheses indicate the number of depressions which intensified into cyclonic storms)

Year	June	July	August	September	Total no. of storms per season
1	2 (2)	5 (3)	2 (1)	2 (1)	11 (7)
2	–	2 (2)	2 (1)	1 (1)	5 (4)
3	–	1 (1)	3 (1)	2 (2)	6 (4)
4	–	2 (–)	1 (–)	2+1[a](1)	6 (1)
5	–	4 (–)	5 (2)	1 (–)	10 (2)
Total no. of storms	2 (2)	14 (6)	13 (5)	9 (5)	38 (18)
Mean per year	0.4 (0.4)	2.8 (1.2)	2.6 (1)	1.8 (1)	7.6 (3.6)

[a]Mid-tropospheric cyclone over the Arabian Sea

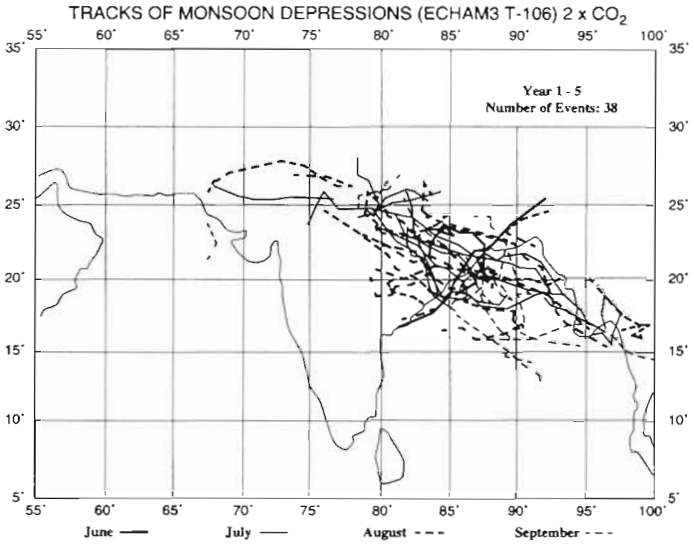

Fig. 16. Tracks of monsoon depressions for June to September as simulated by the model during Years 1 to 5 of the doubled CO_2 experiment

doubled CO_2 experiment, as opposed to 3 in the control experiment. Nonetheless, considering the large interannual variability in the distribution of depressions over the Arabian Sea, 5 yr of model integration are insufficient to draw a firm inference. The tracks of these monsoon depressions as simulated by the model in the doubled CO_2 experiment are illustrated in Fig. 16. Almost all the depressions developing in July and August followed a northwesterly track while those in September had a tendency to be more variable in their path of movement, as noticed for the disturbances developing in the control simulation. No significant changes in either the lowest central pressure or maximum wind speed were observed for the depressions developing in the 2 × CO_2 experiment relative to the control experiment. Also, fewer depressions intensified into cyclonic storms in the doubled CO_2 experiment as compared to the control experiment. However, the average duration of monsoon depressions in July and August increased by 0.9 and 1.2 d, respectively, in the doubled CO_2 simulation. This could be attributed to an increased source of energy at the warmer and wetter land surface and the higher water-holding capacity of a warmer atmospere.

Upon first consideration it is reasonable to assume that global warming could induce higher sea surface temperatures, which might favour a higher frequency of cyclonic vortices in susceptible locations including the Indian seas. Emanuel (1988), using the concept of the Carnot engine, provided a convincing argument that the maximum possible hurricane intensity in a particular region is related to the sea surface temperature. However, the upper troposphere is expected to warm more than the surface, particularly in the moist tropical atmosphere, due to greenhouse forcing as a consequence of lapse rate-temperature feedback, among other physical processes. Fig. 17 illustrates that the CO_2-induced warming over the north Bay of Bengal is most pronounced from 300 to 200 hPa during the monsoon season. This should enhance the stability of the moist tropical troposphere in a doubled CO_2 atmosphere, thus prohibiting stronger convection and hence intense cyclonic disturbances.

Over Indian seas, there is no change in surface evaporation in a doubled CO_2 atmosphere. The vertical wind shear already present over the region in the control simulation during the monsoon season (which prohibits the intensification of monsoon depressions to hurricanes) also is not found to change considerably in the doubled CO_2 experiment. A comparison of the vertical thermal structure for the control and doubled CO_2 experiments suggests that the tropopause shifts up to a higher level under enhanced CO_2 conditions over the Bay of Bengal. This is supported by the stronger vertical velocities and denser upper tropospheric clouds over the region observed under doubled CO_2 conditions (Fig. 18). However, there is no significant change in the vertical structure of vorticity over the region (Fig. 19). The average

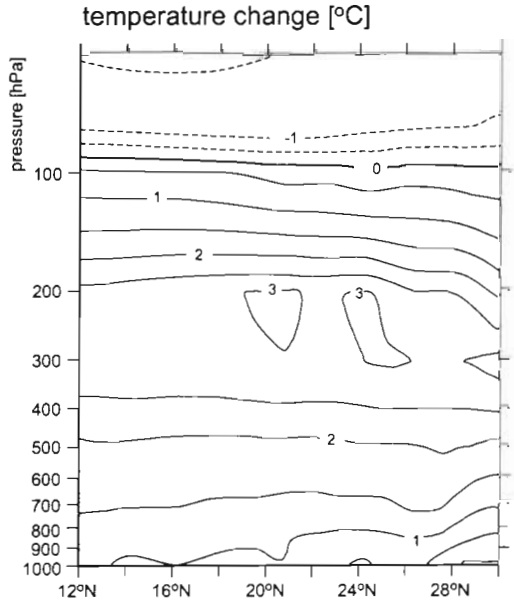

Fig. 17. Change in thermal structure of the atmosphere over the Bay of Bengal (along 90° E longitude) during monsoon season due to doubling of CO_2

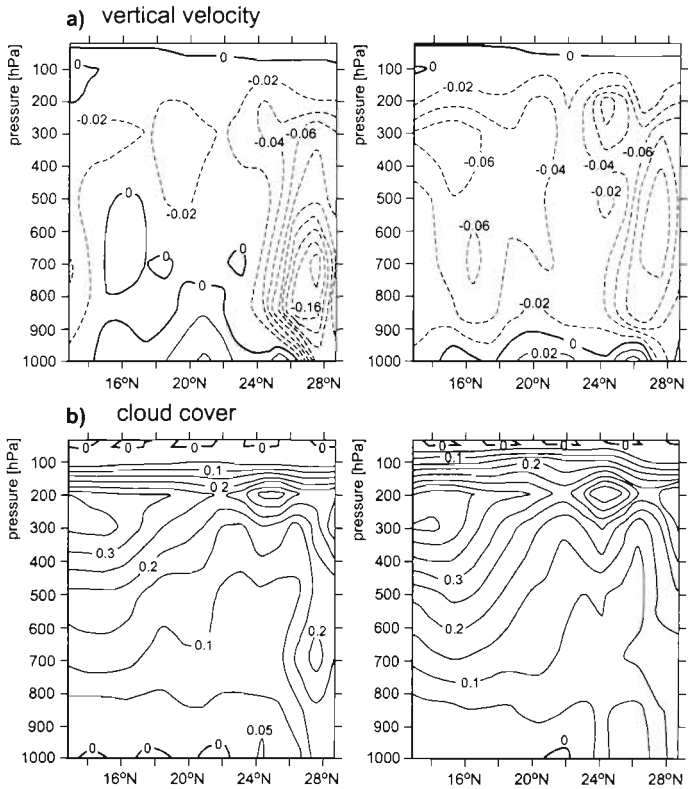

Fig. 18. Vertical distribution of vertical velocities (Pa s^{-1}) and fractional cloud coverage over the Bay of Bengal (along 90° E longitude) during monsoon season in the control (left) and doubled CO_2 (right) simulations

increase in maximum precipitation intensity associated with monsoon depressions is only between 2 and 4.5%. This suggests that no changes are likely in the number and intensity of monsoon depressions in a warmer atmosphere.

CONCLUSIONS

The ECHAM3 model was able to realistically simulate the present-day climate and its seasonal cycle at T106 resolution. For assessing synoptic-scale disturbances under present and doubled CO_2 conditions, 5 yr of model integration is a rather short period, considering the large inherent interannual variability observed in monsoon circulation. Nonetheless, the results presented here clearly demonstrate that high resolution GCMs should be able to simulate the characteristic features of monsoon depressions realistically. Further improvements in the physical parameterization of subgrid-scale processes, e.g. cumulus convection, cloud-radiation interaction and land surface processes, in climate models should improve their skill in simulating the observed rainfall and its variability, particularly for the tropics.

Acknowledgements. The authors are indebted to the Swiss Climate Computing Centre for providing the computational resources for the experiment under a joint cooperative program between the Max Planck Institute for Meteorology in Hamburg and the Eidgenössische Technische Hochschule in Zürich. The experiment was part of the EC Environmental Project under contract No. EV5U-CT92-0123. The first author (M.L.) is grateful to the Deutsches Klimarechenzentrum GmbH (DKRZ) and Max Planck Institute for Meteorology for extending facilities to perform this study. The visit of M.L. to the DKRZ was funded by the German Ministry for Research and Technology (BMFT). The authors thank E. Roeckner, K. Arpe and J. Waszkewitz for helpful suggestions. The assistance of Peter Lenzen in data extraction and analysis is also appreciated. Ms Marion Grunert skilfully drafted the illustrations included in this paper.

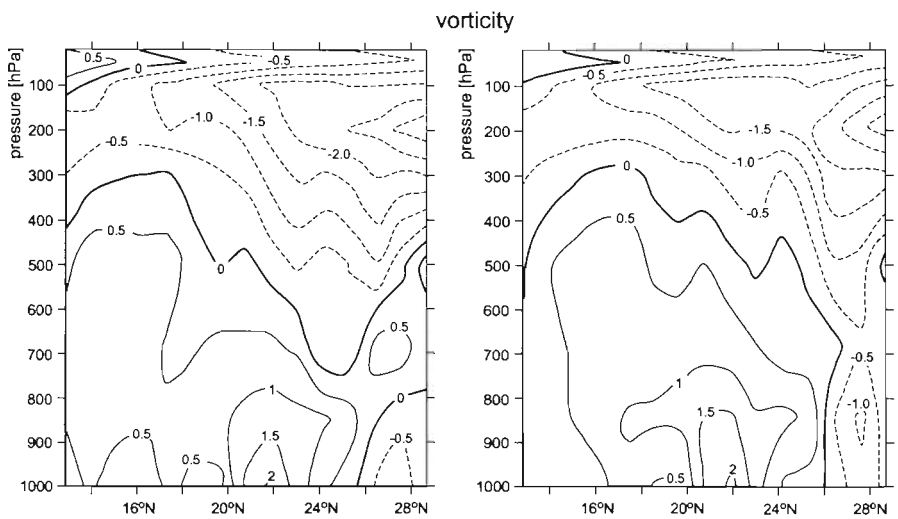

Fig. 19. Vertical distribution of vorticity (10^{-5} s^{-1}) over the Bay of Bengal (along 90° E longitude) during monsoon season in the control (left) and doubled CO_2 (right) simulations

LITERATURE CITED

Arpe K, Bengtsson L, Dümenil L, Roeckner E (1994) The hydrological cycle in the ECHAM3 simulations of the atmospheric circulation. In: Desbois M, Desalmond F (eds) Global precipitation and climate change. NATO ASI Series 26(1):361–377

Bengtsson L, Botzet M, Esch M (1995a) Hurricane-type vortices in a general circulation model. Tellus 47A:175–196

Bengtsson L, Botzet M, Esch M (1995b) Will greenhouse gas-induced warming over the next 50 years lead to higher frequency and greater intensity of hurricanes? Tellus (in press)

Brinkop S (1991) Inclusion of cloud processes in the ECHAM PBL parameterization. Met Inst Univ, Hamburg, Large Scale Atmospheric Modelling Rep No 9:5–14

Cubasch U, Hasselmann K, Höck H, Maier-Reimer E, Mikolajewicz U, Santer BD, Sausen R (1992) Time-dependent greenhouse warming computations with a coupled ocean-atmosphere model. Clim Dyn 8:55–69

Cubasch U, Waszkewitz J, Hegerl G, Perlwitz J (1995) Regional climate changes as simulated in time-slice experiments. Max Planck Institute, Hamburg, Rep No 153

DKRZ (1992) The ECHAM3 atmospheric general circulation model. Deutsches Klimarechenzentrum, Hamburg, Tech Rep No 6

Dümenil L, Todini E (1992) A rainfall-runoff scheme for use in Hamburg GCM. Eur Geophys Soc Ser hydrolog Sci 1: 129–157

ECMWF (1993) The description of the ECMWF/WCRP Level III-A global atmosphere data archive. Technical Attachment of European Centre for Medium Range Weather Forecasts, Shinfield Park, Reading, Berks RG2 9AX, UK

Emanuel KA (1988) Towards a general theory of hurricanes. Am Sci 371–379

Gleckler PJ, Randall DA, Boer G, Colmann R, Dix M, Galin V, Helfand M, Kiehl J, Kitoh A, Lau W, Liang X, Lykossov V, McAvaney B, Miyakoda K, Planton S (1994) Cloud-radiative effects on implied oceanic energy transports as simulated by atmospheric general circulation models. PCMDI Rep No 15, PCMDI/LLNL, Livermore, CA

Godbole RV (1977) The composite structure of the monsoon depression. Tellus 29:25–40

Hense A, Kerschgens M, Raschke E (1982) An economical method for computing radiative transfer in general circulation models. Q J R Meteorol Soc 108:231–252

Joseph PV, Raman PL (1966) Existence of low level westerly jet stream over peninsular India during July. Ind J Met Geophys 17:407–410

Keshavamurty RN, Sankar Rao M (1992) The physics of monsoons. Allied Publishers Ltd, New Delhi

Lal M (1993) Simulation of present-day monsoon rainfall climatology with ECHAM model: impact of physical parameterisation and resolution. In: Boer GJ (ed) WMO/CAS-WGNE Rep No 18, Research activities in atmospheric and oceanic modelling. WMO-TD No 533, 4.18–4.20

Legates DR, Willmott CJ (1990a) Mean seasonal and spatial variability in global surface air temperature. Theor appl Climatol 41:11–21

Legates DR, Willmott CJ (1990b) Mean seasonal and spatial variability in gauge-corrected global precipitation. J Climatol 10:111–127

Louis JF (1979) A parametric model of vertical eddy fluxes in the atmosphere. Bound Layer Meteorol 17:187–202

Mandal GS (1991) Tropical cyclones and their forecasting and warning systems in the north Indian ocean. WMO Tropical Cyclone Programme Rep No TCP-28, WMO-TD No 430, p 430

Miller FR, Keshavamurthy RN (1968) Structure of an Arabian Sea summer monsoon system. Meteorological Monograph, East-West Centre Press, Hawaii

Miller MJ, Palmer TN, Swinbank R (1989) Parameterization and influence of sub-grid scale orography in general circulation and numerical weather prediction models. Met Atmos Phys 40:84–109

Mulki G, Banerjee AK (1960) The mean upper wind circulation around monsoon depressions in India. J Meteorol 17: 8–14

Palmer TN, Shutts GJ, Swinbank R (1986) Alleviation of a systematic westerly bias in general circulation and numerical weather prediction models through an orographic gravity wave drag parameterization. Q J R Meteorol Soc 112: 1001–1031

Perlwitz J, Cubasch U, Roeckner E (1993) Time-slice climate change experiments. In: Boer GJ (ed) WMO/CAS-WGNE Rep No 18, Research Activities in Atmospheric and Oceanic Modelling. WMO-TD No 533, 9.9

Rao YP (1976) Southwest monsoon. Meteorological Monograph No 1, India Meteorological Department, New Delhi

Rockel B, Raschke E, Weynes B (1991) A parameterization of broad band radiative transfer properties of water, ice and mixed clouds. Beitr Phys Atmos 64:1–12

Roeckner E, Arpe K, Bengtsson L, Brinkop S, Dümenil L, Esch M, Kirk E, Lunkeit F, Ponater M, Rockel B, Sausen R, Schlese U, Schubert S, Windelband M (1992) Simulation of the present-day climate with the ECHAM model: impact of model physics and resolution. Max Planck Institute, Hamburg, Rep No 93

Roeckner E, Rieland M, Keup E (1991) Modelling of cloud and radiation in the ECHAM model. Proc ECMWF/WCRP Workshop on Clouds, Radiative Transfer and Hydrological Cycle, Nov 12–15, 1990. ECMWF, Reading, p 199–222

Sikka DR (1977) Some aspects of the life history, structure and movement of monsoon depressions. Pure appl Geophys 115:1501–1529

Sikka DR, Paul DK (1975) A diagnostic study on the structure of monsoon depression. Proc Geophysical Fluid Dynamics Workshop, Indian Institute of Science, Bangalore, p 136–182

Sundqvist H (1978) A parameterization scheme for non-convective condensation including prediction of cloud water content. Q J R Meteorol Soc 104:677–690

Tiedtke M (1989) A comprehensive mass flux scheme for cumulus parameterization in large scale models. Mon Weather Rev 117:1779–1800

Editor: G. Esser, Gießen, Germany

Manuscript first received: February 9, 1995
Revised version accepted: May 22, 1995